Photocatalytic ultrafiltration membranes based on visible light responsive photocatalyst: a review

Jingli Fu[a,b,†], Xiuju Wang[a,b,†,*], Zhun Ma[c], Hao Wenming[d], Jianye Li[e,*], Zhongpeng Wang[a,b], Liguo Wang[a,b,*]

[a]*Key Laboratory of Water Resources and Environmental Engineering in Universities of Shandong, University of Jinan, Jinan 250022, China, Tel. +86 19953123057; email: chm_wangxj@ujn.edu.cn (X.J. Wang), Tel. +86 13698613168; emails: lgwang666@163.com (L.G. Wang), jinglifu99@163.com (J.L. Fu), chm_wangzp@ujn.edu.cn (Z.P. Wang)*
[b]*School of Water Conservancy and Environment, University of Jinan, Jinan 250022, China*
[c]*College of Chemical and Environmental Engineering, Shandong University of Science and Technology, Qingdao 266590, China, email: mzyxy199@163.com*
[d]*Jinan Shunhe Instrument Equipment Co. Ltd., Jinan 250000, China, email: 15650017188@163.com*
[e]*School of Chemical and Environmental Engineering, Weifang University of Science and Technology, Shouguang 262700, China, Tel. +86 18366301077; email: ljy@techmoris.com*

ABSTRACT

Photocatalytic ultrafiltration membranes have great potential advantages in future-water treatment systems. The preparation of photocatalytic ultrafiltration membranes and the selection of catalysts are the key to the development of photocatalytic ultrafiltration membranes. This paper reviews the research status, removal mechanism of pollutants, module design and applications of photocatalytic ultrafiltration membranes. The metal-doped TiO_2 photocatalytic ultrafiltration membranes, non-metal-doped TiO_2 photocatalytic ultrafiltration membranes, semiconductor-doped TiO_2 photocatalytic ultrafiltration membranes, co-doped TiO_2 photocatalytic ultrafiltration membrans, and non-TiO_2 system photocatalytic ultrafiltration membranes are introduced in detail. At the same time, it summarizes the removal of micro-pollutants in water, treatment of dyes in water, and applications in other aspects, demonstrating its potential for application in various areas of water treatment systems. Finally, the direction of future research is proposed.

Keywords: Visible light responsive photocatalyst; Photocatalytic ultrafiltration membranes; Application

1. Introduction

Various environmental problems such as energy shortages and water pollution are facing severe challenges with the acceleration of industrialization, urbanization and the continuous development of the human economy. Membrane technology, especially ultrafiltration membranes technology is widely used in membrane reactor [1,2], product purification and concentration [3–5], especially drinking water treatment [6,7] and wastewater treatment [8,9], because of its low cost, simple operation, effective elimination of impurities, bacteria and organic pollutants in water. However, the application of ultrafiltration process still has some shortcomings, such as poor stability of the membrane, low mechanical properties of the membrane, low removal efficiency ratio of some natural small molecules and membrane fouling, which limits the application of ultrafiltration membrane technology in some industries. Among them, the problem of membrane

* Corresponding authors.

† These authors contributed equally to this work.

fouling has become a major factor restricting the development of ultrafiltration membrane technology. Therefore, the question of how to improve the removal efficiency of micro-pollutants by ultrafiltration membranes and reduce membrane fouling has become a key issue.

Since 1972, Fujishima and Honda [10] published electrochemical photolysis of water at a semiconductor electrode. Photocatalytic technology has attracted extensive attentions and applications in many fields [11]. Photocatalytic technology is based on the low-cost stable semiconductor materials that can decompose most organic matter and a small amount of inorganic substances under specific light irradiation, thereby reducing the harm of pollutants to the human body and the environment. It has important application prospects in modern energy and environmental green new technologies. Visible light catalysis technology is favored by researchers because it can make full use of solar energy, and has low energy consumption and broad spectrum in the field of photocatalysis. [12–15]. However, the difficulty in recycling and reusing semiconductor particles is an important factor that restricts the development and application of visible light catalysis technology. In order to overcome the disadvantages of ultrafiltration technology and visible light catalysis, researchers combined visible light catalysis with ultrafiltration technology. Photocatalytic ultrafiltration membranes made by coupling ultrafiltration and visible light catalysis have become a new hot spot in recent years [4,16–18].

At present, the photocatalytic materials for photodegradation and photo-disinfection of water pollutants have Ag_3PO_4 [19,20], $BiVO_4$ [21,22], Bi_2WO_6 [23,24], g-C_3N_4 [25], Fe_2O_3 [26,27], CuS [28], Cu_2O [29–31], ZnO [32], CeO_2 [33], ZnS [34], doped modified TiO_2 [35,36], etc. TiO_2 is mainly modified from precious metal loading, cation-doped TiO_2, anion-doped TiO_2, oxygen-deficient TiO_2 and ion implantation [37]. Among them, modified TiO_2 has great potential in research and environmental applications, due to its advantages of low cost, strong chemical stability and non-toxicity [38]. In addition, modified TiO_2 is widely used in energy utilization and air purification [39–42]. Modified TiO_2 is most widely used in visible light catalytic materials. Moreover, photocatalytic ultrafiltration membranes with modified TiO_2 composite photocatalysts as additives are the most widely studied due to modified TiO_2 unique advantages.

Several review papers have been published about photocatalytic membranes or photocatalytic membrane reactors (PMRs). For example, Zhang et al. [43] summarized and discussed the fabrication methods of recently reported photocatalytic membranes. This article introduced photocatalytic membranes from three aspects: membrane materials, inorganic membranes and inorganic-polymer hybrid membranes. Zhang et al. [44] reviewed membrane fouling in PMRs for water and wastewater treatment, and discussed the relationship of photocatalysis with membrane fouling, as well as fouling mechanisms and fouling control strategies in PMRs. Molinari et al. [45] critically examined and discussed the application of different PMR configurations for organic pollutants degradation in water treatment and synthesis of organic compounds. Janssens et al. [46] summarized the removal of pharmaceutical compounds in wastewater by slurry PMR technology. Most of these reviews focused on

the configurations, applications and performances of PMRs [43–46]. However, this article reviews photocatalytic ultrafiltration membranes based on visible light responsive photocatalyst. Photocatalytic ultrafiltration membranes with modified TiO_2 photocatalyst as additive are the most widely studied. At the same time, ion doping and semiconductor recombination have been proven to be a more effective modification method in the modification methods of TiO_2 such as precious metal deposition, semiconductor recombination, surface modification, ion doping, etc. [47]. The present review mainly focuses on the introduction of photocatalytic ultrafiltration membranes based on the ion doping modification and semiconductor composite modification of TiO_2. After that, this article summarizes the removal mechanism of pollutants, module design and applications of photocatalytic ultrafiltration membranes. Finally, the conclusions and recommendations are proposed to give insights into the future development of photocatalytic ultrafiltration membranes.

2. Photocatalytic ultrafiltration membrane materials and their research status

2.1. Metal-doped TiO₂ photocatalytic ultrafiltration membranes

Metal ions replace Ti^{4+} in the TiO_2 lattice in the form of metal ions or are doped by the form of filling in the lattice spaces. Metal ions can introduce lower impurity levels in the TiO_2 band gap, so that the absorption wavelength range of TiO_2 is expanded to the visible range. On the other hand, metal ions can form traps and increase the capture point of TiO_2 electrons and holes, thereby reducing the recombination probability of electrons and holes, and improving the photocatalytic efficiency of TiO_2. The TiO_2 doped with metals such as Fe^{3+}, Ni^{2+}, Cu^{2+}, Mo^{5+}, Rh^{3+}, Pt and Ti/Ag [48–51]. The photocatalytic activity of TiO_2 is significantly improved by doping metal ions [48–50].

Many studies have shown that metal-doped TiO_2 photocatalytic ultrafiltration membranes displayed superior separation performance of pollutants and antifouling properties. Among the above metal-modified TiO_2 photocatalysts, Fe^{3+} and Ti/Ag modified TiO_2 were applied to the photocatalytic ultrafiltration membranes. Wang et al. [52] doped Fe^{3+} into a TiO_2/polysulfone (PSF) casting solution and used phase transformation to produce a photocatalytic composite ultrafiltration membrane. The result showed that the degradation rate of BPA was 92.30% by Fe-doped (Fe-TiO_2) photocatalytic ultrafiltration membrane in visible light irradiation for 180 min. Its mechanical properties and cleaning performance were significantly enhanced compared with TiO_2 photocatalytic ultrafiltration membrane. The BPA removal mechanism by photocatalytic Fe-TiO_2/PSF ultrafiltration membrane is presented in Fig. 1. First of all, BPA molecules aggregate on ultrafiltration membrane inside pores and surface via the electrostatic adsorption [53]. Doping Fe^{3+} narrows the band gap of TiO_2 by introducing impurity or defect energy level, so that prompts its response to visible light [54,55]. Then, the Fe-TiO_2 particles inside the composite membrane cause separation of photo-induced carriers under visible-light irradiation [52]. The electrons jump from valence band (VB) to conduction band to produce photoelectrons (e^-) and holes
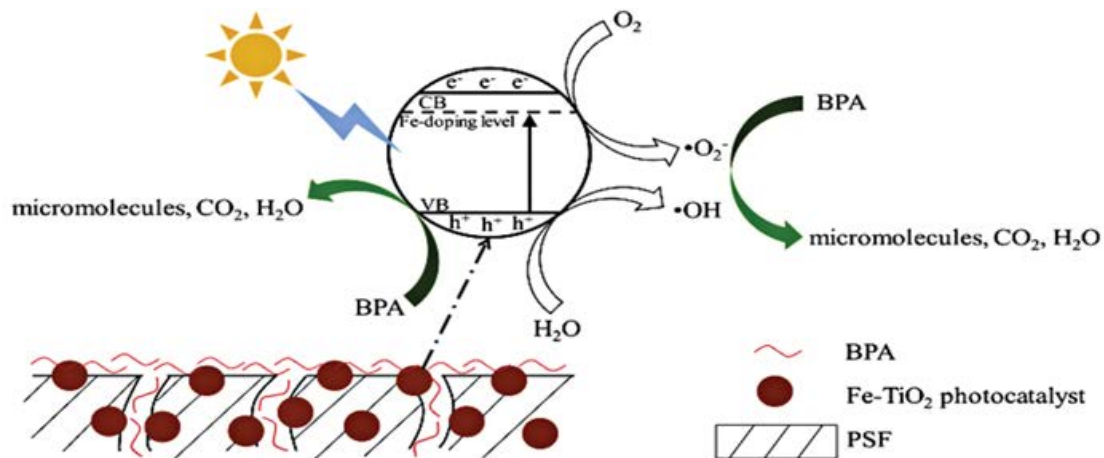
Fig. 1. BPA removal mechanism by photocatalytic Fe-TiO$_2$/PSF composite UF membrane under visible-light irradiation [52].

(h^+). Photoelectrons (e^-) react with O$_2$ to generate free radicals $^•$O$_2^-$, and holes (h^+) react with H$_2$O to generate free radicals $^•$OH. Final, BPA was decomposed into CO$_2$ and H$_2$O by the strong oxidizing radicals and holes [52]. Chun-Yan et al. [56] reported that TiO$_2$ nanoparticle modified with metal Fe was blended with PSF casting solution to prepare uniformly dispersed Fe-TiO$_2$/PSF photocatalytic composite ultrafiltration membrane by LS immersion phase transformation. The result showed that the removal rate of RhB by Fe-TiO$_2$/PSF composite membrane (61%) was significantly higher than that of pure polysulfone membrane (33%) when the mass ratio of Fe-TiO$_2$ to PSF was 0.20. And the membrane hydrophilicity and physicochemical properties were also significantly improved. Lin et al. [51] prepared a new type of TiO$_2$/Ti ceramic-metal composite ultrafiltration membrane by doping silver method. The result indicated that the modification not only overcame the thermal expansion but also increased the stability of thermal dissociation between ceramic membranes. Fig. 2 shows that the FESEM images of supported TiO$_2$/Ti composite tight UF membrane with Ag doping and without Ag doping. The TiO$_2$ membranes by doping Ag presented the homogeneous and integrated surface (Fig. 2a), however the sample without Ag doping presented the surface morphology with acute defects (Fig. 2b) [51]. This can be attributed to that the Ag nanoparticles shows the higher ductility and elastic properties than the TiO$_2$ particles, which can efficiently neutralize and release shrinkage stress during sintering [51]. Moreover, the doping Ag method showed superior photocatalytic performances on dye decomposition [51].

2.2. Non-metallic doped TiO$_2$ photocatalytic ultrafiltration membranes

Non-metallic ions are embedded in the TiO$_2$ lattice, making TiO$_2$ responsive in the visible region by reducing the bandgap of TiO$_2$. Non-metals doped in the TiO$_2$ lattice typically include N, S, C and other non-metallic monomers or their compounds. Some researchers found that the response range of TiO$_2$ materials which were doped with non-metal such as C [57,58], two-dimensional carbon nanomaterials GO [59], N [60], S [61], F [60,62] was successfully extended to the visible light region. Since the atomic radii

of N^{3-} and O^{2-} are close, the N is mainly by occupying the O vacancies in the TiO$_2$ lattice to achieve N-doped TiO$_2$. The interaction between N and O vacancies causes the N2p intermediate level to appear in the forbidden band. On the other hand, N doping is often accompanied by the formation of O vacancies. The formation of N2p intermediate levels and O vacancies lead to the TiO$_2$ response in visible light [63,64]. Doped N is the most studied in the study of non-metallic element doped TiO$_2$ [65].

Among the above non-metal modified TiO$_2$ photocatalysts, the ultrafiltration membranes with two-dimensional carbon nanomaterials graphene oxide or non-metal element N-doped TiO$_2$ as additives is the most widely studied non-metal doped TiO$_2$ photocatalytic ultrafiltration membranes. Studies have shown that graphene oxide or non-metal element N-doped TiO$_2$ photocatalytic ultrafiltration membranes can improve anti-pollution performances and self-cleaning properties [59,66–68]. Pastrana-Martinez et al. [66] prepared the flat sheet photocatalytic ultrafiltration membrane by using lab-made TiO$_2$, graphene oxide-TiO$_2$(GOT), and TiO$_2$ photocatalyst as additives. The research manifested that the membranes prepared with the GOT composite (M-GOT) exhibited the highest photocatalytic activity, outperforming those prepared membranes with bare TiO$_2$ (M-TiO$_2$) and membranes with P25 TiO$_2$ (M-P25) under visible light illumination. Continuous mode experiments proved that the membranes prepared with the GOT composite (M-GOT) had higher pollutant removal efficiency in the near ultraviolet/visible and visible light. This was mainly due to the fact that the GOT has a lower band-gap energy (2.9 eV) than the bare TiO$_2$ (3.2 eV) [66]. Athanasekou et al. [59] synthesized graphene oxide-TiO$_2$ composites and developed a novel visible light responsive catalytic membranes, as the most-efficient material to be used in hybrid photocatalytic/ultrafiltration water treatment processes. Graphene oxide-TiO$_2$ photocatalytic ultrafiltration membrane was proved to be appropriate for the treatment of methylene blue (MB). Zhou et al. [67] synthesized asymmetric N-TiO$_2$ ceramic ultrafiltration membrane via sol-gel method, in which formamide was used as nitrogen resource. As indicated by results, the materials band gap was reduced to 2.65 eV and the absorption band was shifted to about 545 nm. The membrane
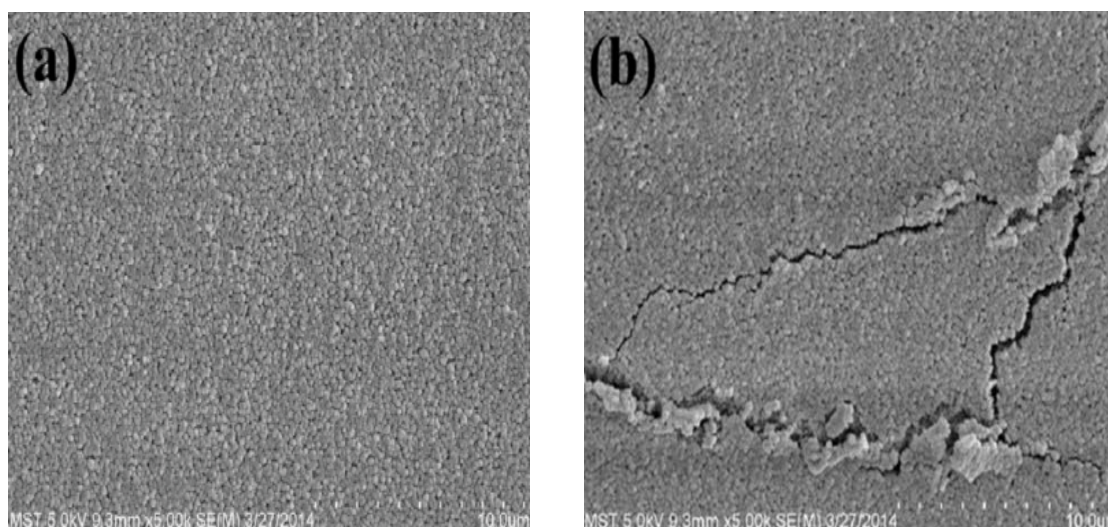
Fig. 2. FESEM images of supported TiO_2/Ti composite tight UF membrane: (a) with Ag doping amount of 6 dwb% and (b) without Ag doping [51].

had excellent visible light absorption and potential application in micro-polluted surface water under visible-light environment. Cheng et al. [68] strived to improve the TiO_2 photocatalytic activity via N-doped TiO_2 used the LPNTP technology under normal pressure and low temperature. The N-doped TiO_2 band gap was reduced to 2.82 eV and the absorption band was shifted to 439 nm. Then, the catalyst was combined with ceramic ultrafiltration membrane. The N-doped TiO_2 photocatalyst recovery efficiency reached 99.5% after the ultrafiltration had been carried out for 90 min and the result indicated that the photocatalyst was able to be separated/recovered completely.

2.3. Semiconductor material doped TiO_2 photocatalytic ultrafiltration membranes

The spectral response of TiO_2 is expanded by doping semiconductor materials into the TiO_2 lattice. The reason is that the band gap of the conductance band and valence band of the two kinds of semiconductors are inconsistent to cause overlap, thereby increasing the separation rate of the photogenerated charge and expanding the spectral response of TiO_2. On the other hand, the composite forbidden band width of two different semiconductor materials is narrower than that of the TiO_2, and the reduction of the forbidden band width can effectively reduce the energy required for light excitation. The research verified that the doping of semiconductor materials such as In_2O_3 [69,70], BiOCl [71], Cu_2O [72], Ag_2O [73], SiO_2 [74,75], g-C_3N_4 [76] and Bi_2MoO_6 [77] not only effectively expanded the visible light absorption range of TiO_2 but also greatly improved the coupling effect between photo-generated electrons and holes, thereby improving photocatalytic performance.

Among the above semiconductor modified TiO_2 photocatalysts, g-C_3N_4 modified TiO_2 was successfully applied to photocatalytic ultrafiltration membranes. The photocatalytic performances and anti-contamination properties of the ultrafiltration membrane can be improved by doping semiconductor material into the TiO_2 as additives. Yu et al. [78]

successfully synthesized nanocomposites using mesoporous graphite carbonitrides (mpg-C_3N_4) and titanium dioxide (TiO_2). The photocatalytic ultrafiltration membrane was prepared by combining mpg-C_3N_4/TiO_2 with polysulfone (PSF) matrix. It can be seen from Fig. 3 that TiO_2 nanospheres adhere to the mesoporous surface of mpg-C_3N_4. Moreover, the authors demonstrated the synthesis of mpg-C_3N_4/TiO_2 and the successful loading of mpg-C_3N_4/TiO_2 within the PSF membrane using EDX elemental analysis spectrum. The research showed that the novel photocatalytic ultrafiltration membrane had good ability to degrade the antibiotic sulfamethoxazole (SMX) in sunlight. The structure of novel mpg-C_3N_4/TiO_2 photocatalytic ultrafiltration membranes was able to provide stable support with high integrity and flexibility after solar irradiation [78]. Chi et al. [79] immobilized g-C_3N_4/TiO_2(CNTO) onto polytetrafluoroethylene ultrafiltration membranes (PTFE UFMs) by plasma-enhanced surface graft technique using polyacrylic acid (PAA) as a bridging agent. The g-C_3N_4/TiO_2 was synthesized via calcination of the mixture of melamine powder and TiO_2 particles. The CNTO/PAA/PTFE UFM is highly resistant to fouling in bovine serum albumin (BSA) solution, and the fouled CNTO/PAA/PTFE UFM show ability to rapidly regenerate visible light irradiation. This was due to intrinsic photocatalytic and hydrophilicity property of CNTO.

2.4. Co-doped TiO_2 photocatalytic ultrafiltration membranes

The TiO_2 is modified by a single element to improve the photocatalytic performance of TiO_2, and its effect is limited. In recent years, the study of co-doping a plurality of substances having different properties with TiO_2 has attracted more and more attention in improving the visible light catalytic activity system of TiO_2. The composite materials formed by co-doping TiO_2 include nitrogen and metal (Fe, Ni, Ag, or Pt)-TiO_2 [80], N-F-TiO_2 [81,82], Ag_3PO_4/TiO_2/Fe_3O_4 [83], N-C-TiO_2 [84], N-Pd-TiO_2 [85], N/GO-TiO_2 [86,87], g-C_3N_4/Ag/TiO_2 [88], etc. The co-doped TiO_2 not only enhances the absorption of visible light by TiO_2 but also helps
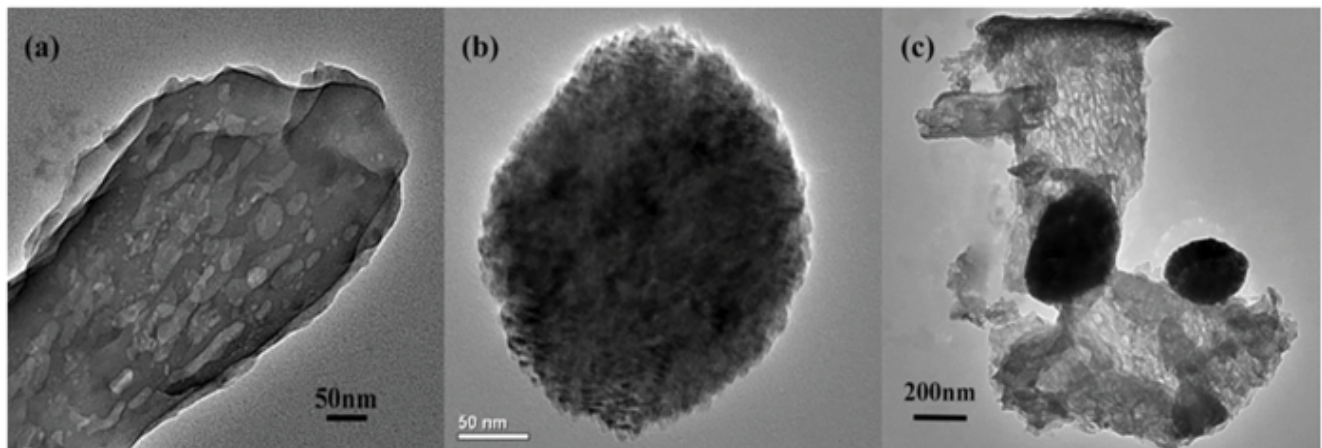
Fig. 3. TEM images of (a) mpg-C_3N_4, (b) TiO_2 nanospheres, and (c) mpg-C_3N_4/TiO_2 [67].

the adsorption of reactants by increasing the surface acidity of TiO_2, thereby further improving photoactivity of TiO_2.

The co-doped TiO_2 photocatalytic ultrafiltration membranes are divided into two categories. One type is TiO_2 doped with the same type of materials photocatalytic ultrafiltration membranes, such as different non-metallic elements co-doped TiO_2 photocatalytic ultrafiltration membranes [84,86,87,89]. Among the above-mentioned photocatalysts of the same type of materials co-doped with TiO_2, N/GO-TiO_2 and N-C-TiO_2 were successfully applied to photocatalytic ultrafiltration membranes. Xu et al. [87] prepared a new graphene oxide derivative (NRG) by doping N into graphene oxide. The graphene oxide derivative (NRG) was combined with the titanium dioxide (TiO_2) nanoparticles to form NRG/TiO_2 (NRGT). The NRG/TiO_2 (NRGT) nanocomposites were introduced into the membrane matrix. The study has indicated that the hydrophilicity of the ultrafiltration membrane was significantly improved, and the rejection rate to the BSA solution and the antifouling property depended on the mixing amount of the NRGT nanocomposite. Then, Xu et al. [89] synthesized N-doped graphene/titania (NRGT) nanocomposites by non-solvent induction method, and doped it into polysulfone (PSF) to synthesize NRGT-PSF membrane. This research has proved that NRGT-PSF membrane exhibited higher photolytic efficiency to methylene blue (MB) at UV light (about 20%–50% improvement) and sunshine (about 30%–80% improvement). And NRGT-PSF membrane can maintain high water flux and good anti-fouling ability after being polluted. Chen et al. [86] discussed a photocatalytic polysulfone ultrafiltration membrane prepared by grafting with N–TiO_2/graphene oxide (NTG). Methylene blue removal under ultraviolet light, darkness and sunlight were used to characterize the photocatalytic ability. The membrane exhibited an enhanced photocatalytic performance, especially in sunlight rather than in ultraviolet light. The kinetics for N–TiO_2/graphene oxide membrane (NTG-M) in sunlight is ~4% faster than in UV, which implies that NTG-M is better utilized in sunlight. The recyclability of the photocatalytic membrane had a great improvement compared with the powder photocatalyst. Cao et al. [84] fabricated a visible-light response mesoporous N, C-co-doped TiO_2 ultrafiltration membrane via a weak alkaline sol–gel process.

The fabrication of visible-light response ultrafiltration membrane demonstrated remarkable photocatalytic activity in visible-light and exhibited extraordinary water permeability.

The other type is TiO_2 doped with a mixture of different types of materials photocatalytic ultrafiltration membranes, such as non-metal and metal co-doped TiO_2 photocatalytic ultrafiltration membranes [85]. Among the above-mentioned photocatalysts of the different types of materials co-doped with TiO_2, N-Pd-TiO_2 was successfully employed to photocatalytic ultrafiltration membranes. Kuvarega et al. [85] reported N, Pd co-doped TiO_2 nanoparticles were successfully embedded in PSF ultrafiltration composite membranes by a simple phase inversion method. This study has presented that the addition of N, Pd-TiO_2 to PSF membranes resulted in the improved membrane wettability, porosity, and visible light activity while membrane integrity was maintained. The higher TiO_2 content resulted in an increase of membrane roughness. The PSF composite membranes by doping 7% N, Pd-TiO_2 can achieve up to 92% dye degradation within 180 min after visible light irradiation.

2.5. Non-TiO_2 system photocatalytic ultrafiltration membranes

The novel non-TiO_2 system visible light responsive photocatalysts mainly include bismuth-base semiconductor materials, oxide type, metallic sulfide and oxyhalogenide visible light responsive photocatalysts, etc. Bismuth-base semiconductor materials mainly include Bi_2O_3 [90], $BiVO_4$ [91], $BiPO_4/Ag_3PO_4$ [92], and $BiOI/Bi_2WO_6$ [93] composite bismuth-base catalysts. The oxide type visible light responsive photocatalysts include photocatalysts such as WO_3 [94,95], γ/α-Fe_2O_3 [96], $Nd_2Zr_2O_7$ [97], $Sm_2Ti_2O_7$ [98], CuO [99], ZnO [100,101], etc. Metallic sulfide photocatalysts mainly include ZnS [102], CuS [103], CdS [104], Ag_2S [105], etc. Oxyhalogenide photocatalysts mainly include BiOX (X = Cl, Br, I) [106], $PbBiO_2Br$ [107], BiOClBr [108], etc. The photocatalytic properties are not significant when these visible light responsive photocatalyst act alone. However, these single photocatalyst can enhance the activity of the visible light responsive photocatalyst by doping element and photosensitization modification, etc.

There were few studies on non-TiO$_2$ photocatalytic ultrafiltration membranes than TiO$_2$-based photocatalytic ultrafiltration membranes. Among the above non-TiO$_2$ photocatalysts, γ/α-Fe$_2$O$_3$, CU$_2$O, WO$_3$, etc. were successfully applied to photocatalytic ultrafiltration membranes. Zhang et al. [109] studied the α-Fe$_2$O$_3$ nanocrystals were entrapped PVDF membranes because of the high density Fe^{3+} of {210} and {001} planes. The size, morphology and internal structure of α-Fe$_2$O$_3$ nanocrystals are shown in Fig. 4. The structure of the α-Fe$_2$O$_3$ nanocrystals are nanorods with a diameter of 10–15 nm (Fig. 4a) and nanoparticles with a size of 20 nm (Fig. 4b). The results of this research indicated that α-Fe$_2$O$_3$/PVDF membrane showed effective photocatalytic degradation of Congo red (CR) attributed to the higher surface density of Fe^{3+}. At the same time PVDF membrane blended α-Fe$_2$O$_3$ nanorods could enhance their antifouling ability because of the photo-Fenton degradation of CR dye under the visible light irradiation [109]. The α-Fe$_2$O$_3$/PVDF membrane was difficult to find Fe$_2$O$_3$ nanorods because the α-Fe$_2$O$_3$ nanorods are surrounded or dispersed by the polymer, as shown in Fig. 5a. Fig. 5b exhibited that the PVDF membrane had a pore size of 10 mm [109]. Singh et al. [110] explained characterization and synthesis of polysulfone ultrafiltration membranes modified with Cu$_2$O. Ibuprofen (IBP) was used to study the pharmaceutical drug removal by synthesized ultrafiltration membranes. The results indicated that IBP was successfully removed under visible light conditions and the removal rate of IBP was 86% by membrane RY4 with amount of 2.0% Cu$_2$O. The results of this study confirmed that the optimal removal condition was pH 4.5. It was due to the surface charge and electrical properties of IBP. IBP is a weak acid with pKa values in between 4.52 and 4.9 resulted with IBP exists as an electrically neutral species under weak acidic conditions, whereas, the Cu$_2$O was present as a positive charge containing species. These reasons facilitated the adsorption of IBP in the membranes and catalyst surface [110,111]. Kazemi et al. [112] developed the WO$_3$ nanostructures modified by doping with iron. The photocatalytic ultrafiltration membranes were prepared using Fe^0-doped WO$_3$ photocatalytic nanoparticles via layer by layer technology. The novel PES ultrafiltration membranes have shown significant Cr(VI) ions removal under visible-light illumination. Ramanan et al. [113] demonstrated that photo-mobile 4,4-azodianiline(AZO) and a bio-adhesive polydopamine (PDA) were co-deposited onto UF membrane surface. AZO undergoes photoisomerization from the cis- to trans- configuration under visible light condition, and the self-cleaning behavior of the modified membranes was due to the reversible volume change.

3. Removal mechanism of pollutants and membrane module design

3.1. Removal mechanism of pollutants by photocatalytic ultrafiltration membranes

The photodegradation mechanism of pollutants by photocatalytic membranes is proposed and is shown in Fig. 6. First of all, pollutants aggregate on ultrafiltration membranes inside pores and surface via the electrostatic adsorption [53]. The membrane with photocatalyst loading showed the better photodegradation performance, and this is due to ultrafiltration membrane had high thermal, and chemical resistance that can support photocatalyst to generate radicals to degrade the contaminants [114]. Doping metal, etc. narrows the band gap of TiO$_2$ by introducing impurity or defect energy level [54,55], and the charge transfer can be achieved in photocatalyst system under visible light irradiation [115]. Then this causes modified TiO$_2$ (m-TiO$_2$) to generate holes (h$^+$) and electrons (e$^-$) under visible light irradiation (Eq. (1)). The holes (h$^+$) react with OH$^-$ produced by water molecules (H$_2$O), which is adsorbed on the m-TiO$_2$ surface, to generate hydroxyl radicals (OH$^\bullet$) (Eqs. (2) and (3)). The generated electrons can react with absorbed surface O$_2$ to produce reactive oxygen species (Eq. (4)) [116]. Reactive oxygen species can react with hydrogen ions (H$^+$) to form hydroxyl radicals (OH$^\bullet$) (Eqs. (5)–(7)). Finally, pollutants can be oxidized by the hydroxyl radicals to carbon dioxide and water (Eq. (8)).
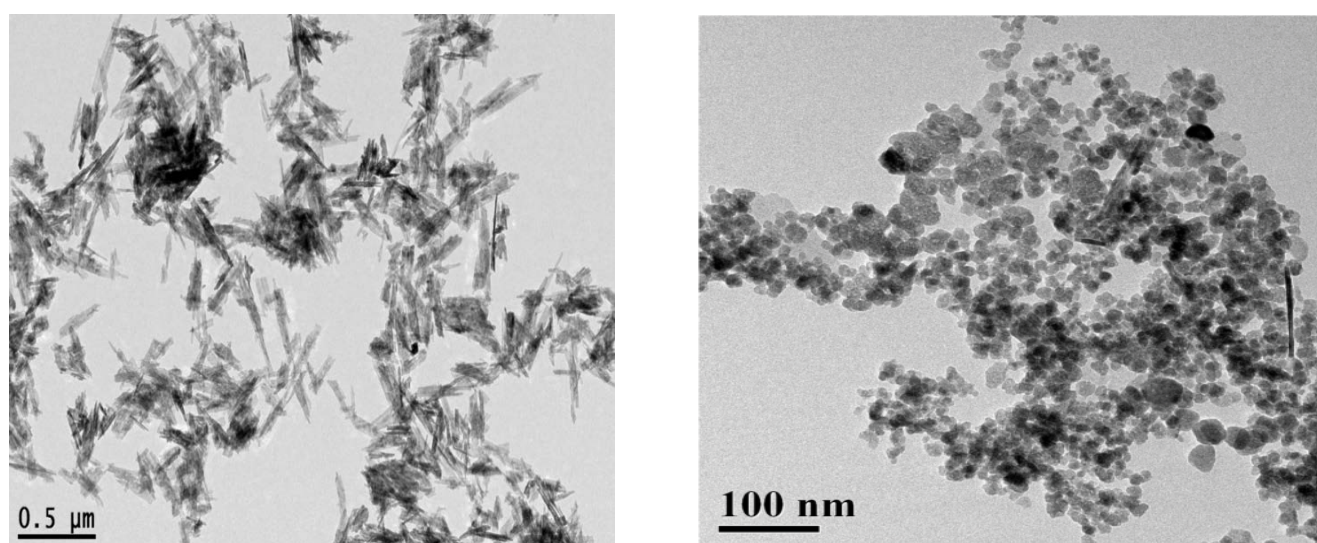
Fig. 4. TEM images of α-Fe$_2$O$_3$ samples: (a) nanorods and (b) nanoparticles [109].
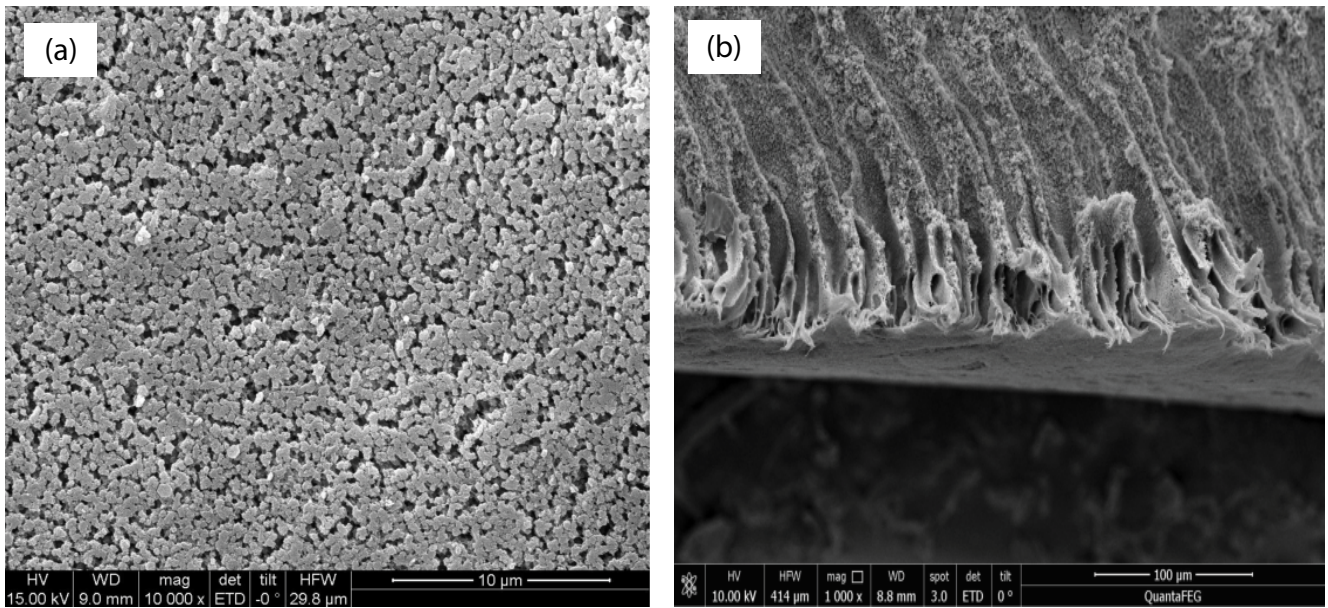
Fig. 5. SEM image of the composited α-Fe$_2$O$_3$/PVDF membrane: (a) surface and (b) cross section [109].
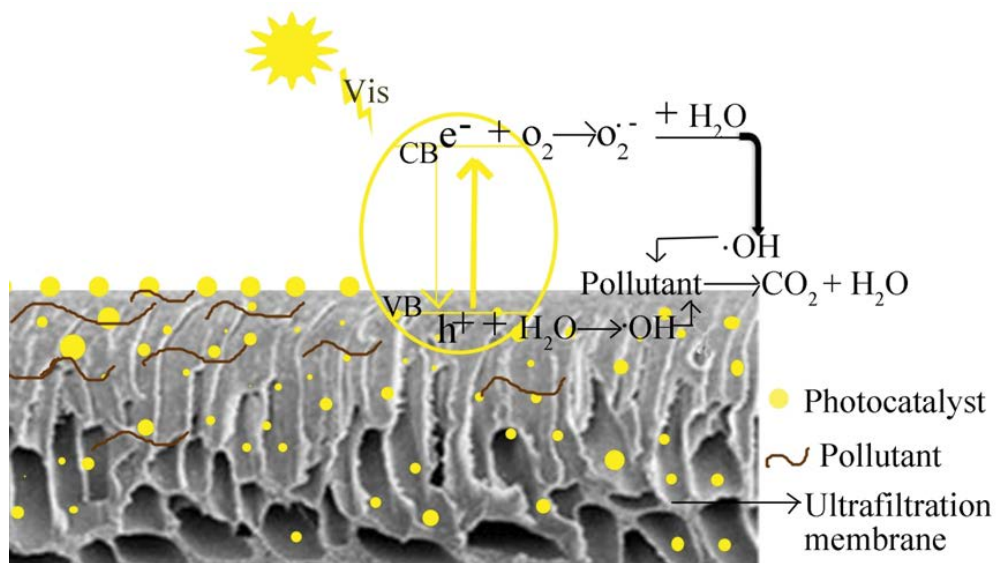
Fig. 6. Pollutions removal mechanism by photocatalytic ultrafiltration membrane under visible-light irradiation.

Meanwhile, hydroxyl radical can also inactivate microorganisms, bacteria and viruses [11].

$$m\text{-}TiO_2 \xrightarrow{h\gamma} h^+ + e^- \tag{1}$$

$$H_2O \rightarrow H^+ + OH^- \tag{2}$$

$$h^+ + OH^- \rightarrow HO^\bullet \tag{3}$$

$$e^- + O_2 \rightarrow O_2^- \tag{4}$$

$$O_2^- + H^+ \rightarrow HO_2^\bullet \tag{5}$$

$$2HO_2^\bullet \rightarrow O_2 + H_2O_2 \tag{6}$$

$$H_2O_2 + h\nu \rightarrow 2HO^\bullet \tag{7}$$

$$Pollutants + HO^\bullet + O_2 \rightarrow intermediates \rightarrow CO_2 + H_2O + \cdots \tag{8}$$
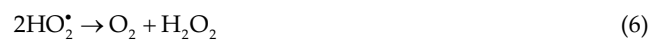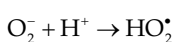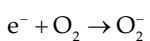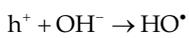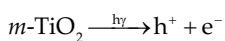
3.2. Photocatalytic ultrafiltration membrane module design

The treatment of wastewater by photocatalytic ultrafiltration membranes is mainly carried out through a PMR [11,117]. The composition and design of the PMR applied in wastewater treatment is presented in Fig. 7. It was generally
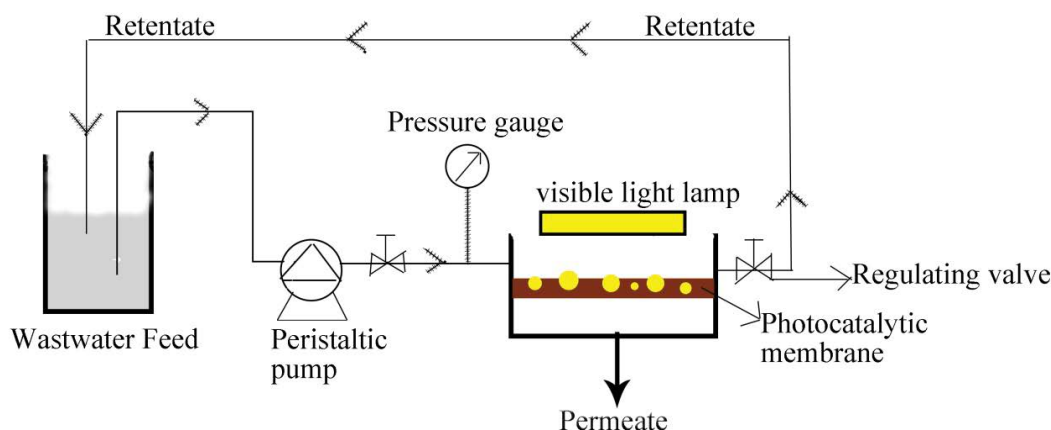
Fig. 7. Configurations of photocatalytic ultrafiltration membrane reactors.

equipped with a light transmissive membrane module and visible-light lamp (or sunlight). The photocatalytic ultrafiltration membrane was fixed on the light transmissive membrane module. The wastewater feed was pumped using a peristaltic pump equipped with a pressure dampener. The retentate was continuously recycled to the wastewater feed tank. Meanwhile, the regulating valve is used to adjust the pressure in order to maintain a constant the transmembrane pressure (TMP) in PMR system.

Key factors affecting the efficiency of PMRs include equipment and system factors. Equipment and system factors mainly include light source [50,52], membrane materials [52,79], photocatalyst type [85,86], and initial pH of solution, and so on. The light source mainly includes xenon lamps, LED lights, solar light, etc. [50,52,78]. The membrane materials mainly include polysulfone, poly ethersulfone, polyvinylidene fluoride, polytetrafluoroethylene and ceramic membrane, etc [52,59,79,109]. The photocatalyst type is mainly the photocatalyst based on modified TiO_2 and non-TiO_2 system photocatalyst [78,89,109]. The initial pH can affect the solubility of the ions such as Ca^{2+} and Mg^{2+} in the solution which in turn affects the efficiency of the PMR [110,111,118].

4. Application of photocatalytic ultrafiltration membranes

Photocatalytic ultrafiltration technology not only overcomes the shortcomings of semiconductor materials that are difficult to recycle and reuse, but also overcomes the membrane fouling and other drawbacks of ultrafiltration membrane technology [119,120]. It makes the photocatalytic ultrafiltration technology to be applied in many areas of water treatment, such as the removal of natural micro-pollutants in the water, the treatment of water dyes, etc. [31,45,121–125]. Pollutants removal by photocatalytic ultrafiltration membranes are shown in Table 1.

4.1. Removal of micro-pollutants

Photocatalytic ultrafiltration membranes were extensively studied for the removal of micro-pollutants. The model micro-pollutants studied to date include diphenhydramine (DP), antibiotic sulfamethoxazole (SMX), ibuprofen

(IBP), diclofenac (DCF) of micro-polluting drug and humic acid (HA), etc. [66,78,110,126,127]. Pastrana-Martinez et al. [66] prepared graphene oxide-TiO_2 membrane (M-/GOT). The membrane was tested in continuous operation mode for the degradation and mineralization of a pharmaceutical compound diphenhydramine (DP) under visible light irradiation, and 61% of diphenhydramine was degraded by the membrane (M-GOT). Yu et al. [78] successfully achieved to degrade the antibiotic sulfamethoxazole (SMX) via novel mpg-C_3N_4/TiO_2 nanocomposite photocatalytic membrane under solar light. 69% of SMX was degraded by the membrane (with 1% mpg-C_3N_4/TiO_2 loading) PSf-3 over the 30 h consecutive solar light irradiation. The pharmaceutically active compound SMX molecule was degraded into seven intermediates of different molecular weights smaller compounds [78]. Singh et al. [110] investigated the degradation of ibuprofen (IBP) through Cu_2O photocatalyst modified polysulfone mixed matrix ultrafiltration membranes under visible light condition. Plakas et al. [126] proposed and evaluated a new type of automatic PMR test device for the degradation of diclofenac (DCF). This research has shown that the catalyst loading significantly affected the removal of DCF under the specific conditions tested. However, hydraulic retention time (HRT) had a rather insignificant effect and revealed the reaction pathways leading to the mineralization of DCF. Szymański et al. [127] indicated that the PMR that is composed of ceramic TiO_2 ultrafiltration membrane had obvious removal of humic acid. And the study had revealed that the membrane fouling can be avoided by an increase of TiO_2 loading from 0.5 to 1.5 g/dm³ in case of model solution of HA. Moreover, the addition of Ca^{2+} and Mg^{2+} to the feed water was able to improve the removal efficiency of HA and reduce membrane fouling. The reason was that Ca^{2+} and Mg^{2+} ions can act as bridges between HA molecules and the surface of the photocatalyst [118]. This led to an increase of adsorption of HA molecules on the surface of TiO_2 particles and thus an improvement of the effectiveness of HA removal from wastewater [127].

4.2. Waste dye water treatment

Removing dyes in wastewater via photocatalytic ultrafiltration membranes has been shown to be more efficient

Table 1
Pollutants removal by photocatalytic ultrafiltration membranes

No	Type of membrane	Pollutant	Pollutants concentration (mg/L)	Degradation time (min)	Pollutant removal	Lamp	Reference
1	Fe-TiO$_2$-PSF	Bisphenol A	10	180	92.30%	Visible-light	[52]
2	Fe-TiO$_2$-PSF	Rhodamine B (RhB)	10	180	61%	500 W xenon lamp	[56]
3	Ag-TiO$_2$/Ti-ceramic–metallic	Rhodamine	5	180	70%	A 500 W xenon lamp	[51]
4	GO-TiO$_2$-MCE	Diphenhydramine and methyl orange (MO)	–	300–400	61%–65%	Visible light	[66]
5	Novel-TiO$_2$-ceramic	Methylene blue (MB) and methyl orange (MO)	2 and 6.4	–	25.2% and 13.3%	Visible light	[59]
6	N-TiO$_2$-ceramic	Azo dyes AO7	10	960	63%	Germicidal lamps with 419 nm	[68]
7	mpg-C$_3$N$_4$/TiO$_2$-PSF	Sulfamethoxazole (SMX)	10	1,800	69%	Solar light	[78]
8	g-C$_3$N$_4$/TiO$_2$/PAA-PTFE	Methylene blue (MB)	10	100	78%	500 W Xe lamp	[79]
9	N-GO/TiO$_2$-PSF	Methylene blue (MB)	50	120	77.5%	100W fluorescent bulb	[89]
10	N-TiO$_2$/GO-PSF	Methylene blue (MB)	50	300	65%–75%	Sunlight	[86]
11	N, C-doped TiO$_2$	Methyl orange	–	240	~99%	Visible-light 700–420nm	[84]
12	N, Pd-TiO$_2$-PSF	Eosin Yellow	100	240	97.3%	500 W Xenon lamp	[85]
13	α-Fe$_2$O$_3$-PVDF	Congo red (CR)	20	120	80%–90%	150W Xenon arc lamp	[109]
14	Cu$_2$O-PSF	Ibuprofen (IBP)	10	60	86.0%	250W lamp with 390–800nm	[110]
15	(CHI-ALG)$_{3.5}$/Fe^0@WO$_3$-PES	Cr(VI) ions	30–10	250	71.3%–84.9%	300W Xenon lamp	[112]
16	RC/TiO$_2$-0.5	Phenol	40	360	78.8%	White light-emitting diode (LED)	[114]
17	Modified TiO$_2$-γ-alumina	Methylene blue	4.8–6.4 and 1.6–2	200–300	50%–60%	Six visible SMD LEDs	[129]

than conventional wastewater treatment such as sedimentation and coagulation. The model pollutants studied to date mainly include alizarin red, methyl orange and methylene blue [59,84,68,128,129]. Oun et al. [128] have shown that TiO_2 nanoparticles were immobilized on a ceramic ultrafiltration membrane. SEM characterization showed that TiO_2 nanoparticles were densely and uniformly covered on ceramic supporting to form a thin layer of about 4.2 mm thick, resulting in a significant reduction of the average pore size (50 nm) while providing water permeability of $117 \, L \, h^{-1} \, m^2 \, bar^{-1}$. TiO_2 nanoparticle-based tubular UF ceramic membranes designed in this way have been shown to achieve up to 99% removal of alizarin red dye. Cheng et al. [68] combined N-doped TiO_2 photocatalyst with ceramic ultrafiltration membranes to degrade azo dyes, and 63% of azo dyes were degraded after 16 h in a photocatalytic system. Cao et al. [84] fabricated a visible-light response mesoporous N, C-co-doped TiO_2 ultrafiltration membranes. The result indicated that no appreciable degradation of methyl orange (MO) was obtained in dark conditions. But the degradation of methyl orange was nearly completed in 4 h under visible light. Moustakas et al. [129] developed visible light active TiO_2 photocatalytic ultrafiltration membranes coated with modified nanostructured titania (*m*-TiO_2). The modified photocatalytic membranes were incorporated in a water purification photocatalytic reactor in continuous flow filtration conditions and tested for the photocatalytic degradation of methyl orange (MO) and methylene blue (MB) compounds with very promising results [129]. Similarly, Athanasekou et al. [59] synthesized ceramic photocatalytic ultrafiltration membranes that proved to be appropriate for the treatment of methyl orange (MO) and methylene blue (MB).

4.3. Other aspects of the application

Photocatalytic ultrafiltration membranes are used in other areas, such as the removal of phenol and the treatment of heavy metal ions [52,112,114]. Wang et al. [52] achieved the removal of bisphenol A by photocatalytic Fe-TiO_2/PSF composite UF membranes under visible-light irradiation. Mohamed et al. [114] prepared a novel polymer–inorganic UF membrane via incorporation of N-doped anatase/rutile mixed phase TiO_2 nanorods into the cellulose microfiber via phase inversion technique. The photocatalytic membranes exhibited the highest photocatalytic activity in the degradation of phenol under visible light irradiation [114]. Kazemi et al. [112] deposited the (CHI-ALG)$_{3.5}$ bilayers and Fe^0@WO_3 on the polyethersulfone (PES) ultrafiltration membrane surface. The novel PES ultrafiltration membrane was used to degrade Cr(VI) ions. By depositing the (CHI-ALG)$_{3.5}$ bilayers and Fe^0@WO_3 on the ultrafiltration membrane surface, the Cr(VI) rejection for 25 mg/L feed concentration was enhanced from 17% for neat PES to 92.1% for PES/(CHI-ALG)$_{3.5}$/Fe^0@WO_3 membrane [112]. This is due to the Fe^0@WO_3 photocatalysts converted by precipitation and reduction of Cr(VI) ions to Cr(III) form [130].

5. Conclusions and perspectives

The photocatalytic ultrafiltration membranes are divided into metal-doped TiO_2 photocatalytic ultrafiltration membranes, non-metal-doped TiO_2 photocatalytic ultrafiltration membranes, semiconductor-doped TiO_2 photocatalytic ultrafiltration membranes, co-doped TiO_2 photocatalytic ultrafiltration membranes, and non-TiO_2 system are the five kinds of photocatalytic ultrafiltration membranes in this paper. Then its removal mechanism of pollutants, module design and applications in various fields of water treatment system are introduced. In five kinds of photocatalytic ultrafiltration membranes, co-doped TiO_2 photocatalytic ultrafiltration membranes are the most widely studied, followed by non-metallic-doped TiO_2 photocatalytic ultrafiltration membranes. The application in water treatment systems is mainly focused on the removal of micro-pollutants and dye in water.

In the future, the research still needs to solve several problems: (1) at present, the wavelength of visible light is 400–800 nm. More studies are needed to focus on the photocatalytic mechanism in the visible wavelength range in the future research work of photocatalytic ultrafiltration membranes. (2) In the study of photocatalytic ultrafiltration membrane based on visible light responsive photocatalyst, although the wavelength absorption range of photocatalytic ultrafiltration membranes has been increased, more attentions should be paid to the use of modified TiO_2 and other visible light responsive photocatalyst. The modified material will not only lead to the complexity of the preparation methods and the cost increase, but also may pollute the environment, such as the addition of heavy metal ions. Therefore, the future search for economic and environment friendly substances modified TiO_2 photocatalytic ultrafiltration membrane is still research hotspot. (3) Photocatalytic ultrafiltration membranes have not yet been established for large-scale industrial applications. Most studies are still in the stage of laboratory development. This main reason is the compatibility of the casting solution with the photocatalyst and the key factors affecting the efficiency of the PMR have not been completely solved. It is the key to future research to study the formation mechanism of membranes, the control factors of membrane materials and photocatalysts, and establishing a widely used design theory of PMRs.

References

[1] M.F. Tay, C. Liu, E.R. Cornelissen, B. Wu, T.H. Chong, The feasibility of nanofiltration membrane bioreactor (NF-MBR)+reverse osmosis (RO) process for water reclamation: comparison with ultrafiltration membrane bioreactor (UF-MBR)+RO process, Water Res., 129 (2018) 180–189.

[2] Z. Ma, T. Lei, X. Ji, X. Gao, C. Gao, Submerged membrane bioreactor for vegetable oil wastewater treatment, Chem. Eng. Technol., 38 (2015) 101–109.

[3] A. Saxena, B.P. Tripathi, M. Kumar, V.K. Shahi, Membrane-based techniques for the separation and purification of proteins: an overview, Adv. Colloid Interface Sci., 145 (2008) 1–22.

[4] R. Molinari, L. Palmisano, V. Loddo, S. Mozia, A.W. Morawski, 21 - Photocatalytic Membrane Reactors: Configurations, Performance and Applications in Water Treatment and Chemical Production, A. Basile, Ed., Handbook of Membrane Reactors, Reactor Types and Industrial Applications, Vol. 2, Woodhead Publishing Limited, 2013, pp. 808–845, ISBN 978-0-85709-415-5.

[5] C. Emin, E. Kurnia, I. Katalia, M. Ulbricht, Polyarylsulfone-based blend ultrafiltration membranes with combined size and charge selectivity for protein separation, Sep. Purif. Technol., 193 (2018) 127–138.

[6] M. Bhadra, S. Mitra, Advances in Nanostructured Membranes for Water Desalination, Chapter 7, In: Nanotechnology Applications for Clean Water, 2nd ed., Department of Chemistry and Environmental Science, New Jersey Institute of Technology, University Heights, Newark, NJ, USA, 2014, pp. 109–122.

[7] S.H. Jia, Z. Ma, J. Qin, H.S. Si, C.-S. Toh, Inline coagulation–ultrafiltration as the pretreatment for reverse osmosis brine treatment and recovery, Desalination, 365 (2015) 242–249.

[8] K.L. Zhou, X.J. Wang, Z. Ma, X.J. Lu, Z.P. Wang, L.G. Wang, Preparation and characterization of modified polyvinylidene fluoride/2-amino-4-thiazoleacetic acid ultrafiltration membrane for purification of Cr(VI) in water, J. Chem. Eng. Jpn, 51 (2018) 501–506.

[9] X. Wang, K. Zhou, Z. Ma, X. Lu, L. Wang, Z. Wang, X. Gao, Preparation and characterization of novel polyvinylidene fluoride/2-aminobenzothiazole modified ultrafiltration membrane for the removal of Cr(VI) in wastewater, Polymers, 10 (2018) 1–9.

[10] A. Fujishima, K. Honda, Electrochemical photolysis of water at a semiconductor electrode, Nature, 5358 (1972) 238–237.

[11] S. Leong, A. Razmjou, K. Wang, K. Hapgood, X. Zhang, H. Wang, TiO$_2$ based photocatalytic membranes: a review, J. Membr. Sci., 472 (2014) 167–184.

[12] Y. Zhao, N. Hoivik, K. Wang, Recent advance on engineering titanium dioxide nanotubes for photochemical and photoelectrochemical water splitting, Nano Energy, 30 (2016) 728–744.

[13] A.L. Linsebigler, G. Lu, J.T. Yates, Photocatalysis on TiO$_2$ surfaces: principles, mechanisms, and selected results, Chem. Rev., 95 (1995) 735–758.

[14] C.S. Uyguner-Demirel, N.C. Birben, M. Bekbolet, Elucidation of background organic matter matrix effect on photocatalytic treatment of contaminants using TiO$_2$: a review, Catal. Today, 284 (2017) 202–214.

[15] K.Z. Qi, B. Cheng, J.G. Yu, W.K. Ho, A review on TiO$_2$-based Z-scheme photocatalysts, Chin. J. Catal., 38 (2017) 1936–1955.

[16] S. Zhao, W. Yan, M. Shi, Z. Wang, J. Wang, S. Wang, Improving permeability and antifouling performance of polyethersulfone ultrafiltration membrane by incorporation of ZnO-DMF dispersion containing nano-ZnO and polyvinylpyrrolidone, J. Membr. Sci., 478 (2015) 105–116.

[17] C. Liao, P. Yu, J. Zhao, L. Wang, Y. Luo, Preparation and characterization of NaY/PVDF hybrid ultrafiltration membranes containing silver ions as antibacterial materials, Desalination, 272 (2011) 59–65.

[18] D. Darowna, R. Wróbel, A.W. Morawski, S. Mozia, The influence of feed composition on fouling and stability of a polyethersulfone ultrafiltration membrane in a photocatalytic membrane reactor, Chem. Eng. J., 310 (2017) 360–367.

[19] G. Ming, Z. Na, Y. Zhao, L. Jing, L. Lu, Sunlight-assisted degradation of dye pollutants in Ag$_3$PO$_4$ suspension, Ind. Eng. Chem. Res., 51 (2012) 5167–5173.

[20] Q. Liang, W. Ma, Y. Shi, Z. Li, X. Yang, Hierarchical Ag$_3$PO$_4$ porous microcubes with enhanced photocatalytic properties synthesized with the assistance of trisodium citrate, Cryst Eng Comm, 14 (2012) 2966–2973.

[21] S. Tokunaga, H. Kato, A. Kudo, Selective preparation of monoclinic and tetragonal BiVO$_4$ with scheelite structure and their photocatalytic properties, Chem. Mater., 33 (2002) 8–9.

[22] J. Yu, A. Kudo, Effects of structural variation on the photocatalytic performance of hydrothermally synthesized BiVO$_4$, Adv. Funct. Mater., 16 (2010) 2163–2169.

[23] C. Zhang, Y. Zhu, Synthesis of square Bi$_2$WO$_6$ nanoplates as high-activity visible-light-driven photocatalysts, Chem. Mater., 17 (2010) 3537–3545.

[24] J. Tang, Z. Zou, J. Ye, Photocatalytic decomposition of organic contaminants by Bi$_2$WO$_6$ under visible light irradiation, Catal. Lett., 92 (2004) 53–56.

[25] X. Wang, K. Maeda, A. Thomas, K. Takanabe, G. Xin, J.M. Carlsson, K. Domen, M. Antonietti, A metal-free polymeric photocatalyst for hydrogen production from water under visible light, Nat. Mater., 8 (2009) 76–80.

[26] Z. Miao, S. Tao, Y. Wang, Y. Yu, C. Meng, Y. An, Hierarchically porous silica as an efficient catalyst carrier for high performance vis-light assisted Fenton degradation, Microporous Mesoporous Mater., 176 (2013) 178–185.

[27] J.Z. Yao, C.L. Li, L.N. Lu, L.W. Bing, A facile and low-cost synthesis of granulated blast furnace slag-based cementitious material coupled with Fe$_2$O$_3$ catalyst for treatment of dye wastewater, Appl. Catal., B, 138–139 (2013) 9–16.

[28] V.K. Gupta, D. Pathania, S. Agarwal, P. Singh, Adsorptional photocatalytic degradation of methylene blue onto pectin–CuS nanocomposite under solar light, J. Hazard. Mater., 243 (2012) 179–186.

[29] H. Huang, J. Zhang, L. Jiang, Z. Zang, Preparation of cubic Cu$_2$O nanoparticles wrapped by reduced graphene oxide for the efficient removal of rhodamine B, J. Alloys Compd., 718 (2017) 112–115.

[30] C. Kong, B. Ma, K. Liu, W. Zhang, Z. Yang, Continuous UV irradiation synthesis of ultra-small Au nanoparticles decorated Cu$_2$O with enhanced photocatalytic activity, Compos. Commun., 9 (2018) 27–32.

[31] M. Aslam, G. Gopakumar, T.L. Shoba, I.S. Mulla, K. Vijaya-mohanan, S.K. Kulkarni, J. Urban, W. Vogel, Formation of Cu and Cu$_2$O nanoparticles by variation of the surface ligand: preparation, structure, and insulating-to-metallic transition, J. Colloid Interface Sci., 255 (2002) 79–90.

[32] M. Montero-Munoz, J.E. Ramos-Ibarra, J.E. Rodriguez-Paez, M.D. Teodoro, G.E. Marques, A.R. Sanabria, P.C. Cajas, C.A. Paez, B. Heinrichs, J.A.H. Coaquira, Role of defects on the enhancement of the photocatalytic response of ZnO nanostructures, Appl. Surf. Sci., 448 (2018) 646–654.

[33] X.P. Li, Y.L. Sun, C.W. Luo, Z.S. Chao, UV-resistant hydrophobic CeO$_2$ nanomaterial with photocatalytic depollution performance, Ceram. Int., 44 (2018) 13439–13443.

[34] Z.Y. Ye, L.Y. Kong, F. Chen, Z.G. Chen, Y. Lin, C.B. Liu, A comparative study of photocatalytic activity of ZnS photocatalyst for degradation of various dyes, Optik, 164 (2018) 345–354.

[35] X. He, Y. Cai, H. Zhang, C. Liang, Photocatalytic degradation of organic pollutants with Ag decorated free-standing TiO$_2$ nanotube arrays and interface electrochemical response, J. Mater. Chem., 21 (2010) 475–480.

[36] B. Naik, M.K. Sun, H.J. Chan, Y.M. Song, H.K. Sang, J.Y. Park, Enhanced H$_2$ generation of Au-loaded, nitrogen-doped TiO$_2$ hierarchical nanostructures under visible light, Adv. Mater. Interfaces, 1 (2014)1–6.

[37] N. Rahimi, R.A. Pax, E.M. Gray, Review of functional titanium oxides. I: TiO$_2$ and its modifications, Prog. Solid State Chem., 44 (2016) 86–105.

[38] A.J. Haider, R.H. Al-Anbari, G.R. Kadhim, C.T. Salame, Exploring potential environmental applications of TiO$_2$ nanoparticles, Energy Procedia, 119 (2017) 332–345.

[39] S.S. Arbuj, Synthesis of nanostructured TiO$_2$ photocatalyst for H$_2$ generation, J. Nanoeng. Nanomanuf., 5 (2015) 232–238.

[40] Z. Junbo, T. Jianli, T. Lin, G. Maochu, Z. Liu, C. Yaoqiang, Photocatalytic degradation of gaseous benzene over TiO$_2$/Sr$_2$CeO$_4$: kinetic model and degradation mechanisms, J. Hazard. Mater., 139 (2007) 323–331.

[41] Z. Shayegan, C.-S. Lee, F. Haghighat, TiO$_2$ photocatalyst for removal of volatile organic compounds in gas phase – a review, Chem. Eng. J., 334 (2018) 2408–2439.

[42] J. Kim, D. Monllor-Satoca, W. Choi, Simultaneous production of hydrogen with the degradation of organic pollutants using TiO$_2$ photocatalyst modified with dual surface components, Energy Environ. Sci., 5 (2012) 7647–7656.

[43] X. Zhang, D.K. Wang, J.C.D. da Costa, Recent progresses on fabrication of photocatalytic membranes for water treatment, Catal. Today, 230 (2014) 47–54.

[44] W. Zhang, L. Ding, J. Luo, M.Y. Jaffrin, B. Tang, Membrane fouling in photocatalytic membrane reactors (PMRs) for water and wastewater treatment: a critical review, Chem. Eng. J., 302 (2016) 446–458.

[45] R. Molinari, C. Lavorato, P. Argurio, Recent progress of photocatalytic membrane reactors in water treatment and in synthesis of organic compounds. A review, Catal. Today, 281 (2017) 144–164.

[46] R. Janssens, M.K. Mandal, K.K. Dubey, P. Luis, Slurry photocatalytic membrane reactor technology for removal of pharmaceutical compounds from wastewater: towards cytostatic drug elimination, Sci. Total Environ., 612 (2017) 599–600.

[47] F. Chen, W. Zou, W. Qu, J. Zhang, Photocatalytic performance of a visible light TiO_2 photocatalyst prepared by a surface chemical modification process, Catal. Commun., 10 (2009) 1510–1513.

[48] A.V. Rosario, E.C. Pereira, The role of Pt addition on the photocatalytic activity of TiO_2 nanoparticles: the limit between doping and metallization, Appl. Catal., B, 144 (2014) 840–845.

[49] S.N.R. Inturi, T. Boningari, M. Suidan, P.G. Smirniotis, Visible-light-induced photodegradation of gas phase acetonitrile using aerosol-made transition metal (V, Cr, Fe, Co, Mn, Mo, Ni, Cu, Y, Ce, and Zr) doped TiO_2, Appl. Catal., B, 144 (2014) 333–342.

[50] S.A. Ibrahim, M.N. Ahmid, Influence of calcination temperature towards Fe-TiO_2 for visible-driven photocatalyst, Mater. Sci. Forum, 888 (2017) 435–440.

[51] Y. Lin, Y. Cai, E. Drioli, Y. Fan, Enhancing mechanical and photocatalytic performances on TiO_2/Ti composite ultrafiltration membranes via Ag doping method, Sep. Purif. Technol., 145 (2015) 29–38.

[52] Q. Wang, C. Yang, G. Zhang, L. Hu, P. Wang, Photocatalytic Fe-doped TiO_2/PSF composite UF membranes: characterization and performance on BPA removal under visible-light irradiation, Chem. Eng. J., 319 (2017) 39–47.

[53] Z. Xu, S. Ye, G. Zhang, W. Li, C. Gao, C. Shen, Q. Meng, Antimicrobial polysulfone blended ultrafiltration membranes prepared with Ag/Cu_2O hybrid nanowires, J. Membr. Sci., 509 (2016) 83–93.

[54] H.R. Rajabi, O. Khani, M. Shamsipur, V. Vatanpour, High-performance pure and Fe^{3+}-ion doped ZnS quantum dots as green nanophotocatalysts for the removal of malachite green under UV-light irradiation, J. Hazard. Mater., 250–251 (2013) 370–378.

[55] W. Zhao, Z. Jing, G. Zhang, L. Xi, H. Wu, Z. Hao, Controlled synthesis of $Zn_{(1-1.5x)}Fe_xS$ nanoparticles *via* a microwave route and their photocatalytic properties, RSC Adv., 5 (2015) 106644–106650.

[56] Y. Chun-Yan, W. Qiao, Z. Guang-Shan, W. Peng, Preparation of photocatalytic composite ultrafiltration membrane and its properties under simulated solar irradiation, Chin. Environ. Sci., 12 (2017) 4564–4570.

[57] X. Wang, S. Meng, X. Zhang, H. Wang, W. Zhong, Q. Du, Multi-type carbon doping of TiO_2 photocatalyst, Chem. Phys. Lett., 444 (2007) 292–296.

[58] Z. Ying, Z. Zhao, J. Chen, C. Li, J. Chang, W. Sheng, C. Hu, S. Cao, C-doped hollow TiO_2 spheres: in situ synthesis, controlled shell thickness, and superior visible-light photocatalytic activity, Appl. Catal., B, 165 (2015) 715–722.

[59] C.P. Athanasekou, N.G. Moustakas, S. Morales-Torres, L.M. Pastrana-Martínez, J.L. Figueiredo, J.L. Faria, A.M.T. Silva, J.M. Dona-Rodriguez, G.E. Romanos, P. Falaras, Ceramic photocatalytic membranes for water filtration under UV and visible light, Appl. Catal., B, 178 (2015) 12–19.

[60] M. Behpour, R. Foulady-Dehaghi, N. Mir, Considering photocatalytic activity of N/F/S-doped TiO_2 thin films in degradation of textile waste under visible and sunlight irradiation, Sol. Energy, 158 (2017) 636–643.

[61] X. Chen, D.-H. Kuo, D. Lu, Visible light response and superior dispersed S-doped TiO_2 nanoparticles synthesized via ionic liquid, Adv. Powder Technol., 28 (2017) 1213–1220.

[62] M. Pelaez, A.A. de la Cruz, E. Stathatos, P. Falaras, D.D. Dionysiou, Visible light-activated N-F-codoped TiO_2 nanoparticles for the photocatalytic degradation of microcystin-LR in water, Catal. Today, 144 (2009) 19–25.

[63] R. Silveyra, L. De La Torre Sáenz, W.A. Flores, V.C. Martínez, A.A. Elguézabal, Doping of TiO_2 with nitrogen to modify the interval of photocatalytic activation towards visible radiation, Catal. Today, 107 (2005) 602–605.

[64] Y. Nakano, T. Morikawa, T. Ohwaki, Y. Taga, Deep-level optical spectroscopy investigation of N-doped TiO_2 films, Appl. Phys. Lett., 86 (2005) 132104.

[65] A. Nambu, J. Graciani, J.A. Rodriguez, Q. Wu, E. Fujita, S. J Fdez, N doping of TiO_2(110): photoemission and density-functional studies, J. Chem. Phys., 125 (2006) 094706.

[66] L.M. Pastrana-Martínez, S. Morales-Torres, J.L. Figueiredo, J.L. Faria, A.M.T. Silva, Graphene oxide based ultrafiltration membranes for photocatalytic degradation of organic pollutants in salty water, Water Res., 77 (2015) 179–190.

[67] Z. Zhou, W.G. Wang, W. Huang, W.H. Jing, W.H. Xing, Fabrication of mesoporous N-TiO_2 membrane and its spectral characteristics, Adv. Mater. Res., 79–82 (2009) 791–794.

[68] H.-H. Cheng, S.-S. Chen, Y.-W. Cheng, W.-L. Tseng, Y.-H. Wang, Liquid-phase non-thermal plasma-prepared N-doped TiO_2 for azo dye degradation with the catalyst separation system by ceramic membranes, Water Sci. Technol., 62 (2010) 1060–1066.

[69] F. Petronella, S. Rtimi, R. Comparelli, R. Sanjines, C. Pulgarin, M.L. Curri, J. Kiwi, Uniform TiO_2/In_2O_3 surface films effective in bacterial inactivation under visible light, J. Photochem. Photobiol., A, 279 (2014) 1–7.

[70] Z. Jiang, D. Jiang, Z. Yan, D. Liu, K. Qian, J. Xie, A new visible light active multifunctional ternary composite based on TiO_2–In_2O_3 nanocrystals heterojunction decorated porous graphitic carbon nitride for photocatalytic treatment of hazardous pollutant and H_2 evolution, Appl. Catal., B, 170–171 (2015) 195–205.

[71] D. Sánchez-Rodríguez, M.G.M. Medrano, H. Remita, V. Escobar-Barrios, Photocatalytic properties of BiOCl-TiO_2 composites for phenol photodegradation, J. Environ. Chem. Eng., 6 (2018) 1601–1612.

[72] Y. Bessekhouad, D. Robert, J.-V. Weber, Photocatalytic activity of Cu_2O/TiO_2, Bi_2O_3/TiO_2 and $ZnMn_2O_4$/TiO_2 heterojunctions, Catal. Today, 101 (2005) 315–321.

[73] N. Wei, H. Cui, Q. Song, L. Zhang, X. Song, K. Wang, Y. Zhang, J. Li, J. Wen, J. Tian, Ag_2O nanoparticle/TiO_2 nanobelt heterostructures with remarkable photo-response and photocatalytic properties under UV, visible and near-infrared irradiation, Appl. Catal., B, 198 (2016) 83–90.

[74] W. Chang, L. Yan, B. Liu, R. Sun, Photocatalyic activity of double pore structure TiO_2/SiO_2 monoliths, Ceram. Int., 43 (2017) 5881–5886.

[75] A. Pal, T.K. Jana, K. Chatterjee, Silica supported TiO_2 nanostructures for highly efficient photocatalytic application under visible light irradiation, Mater. Res. Bull., 76 (2016) 353–357.

[76] D. Dvoranova, M. Mazur, I. Papailias, T. Giannakopoulou, C. Trapalis, V. Brezová, EPR investigations of G-C_3N_4/TiO_2 nanocomposites, Catalysts, 8 (2018) 47.

[77] J. Tian, P. Hao, N. Wei, H. Cui, H. Liu, 3D Bi_2MoO_6 Nanosheet/TiO_2 nanobelt heterostructure: enhanced photocatalytic activities and photoelectochemistry performance, ACS Catal., 5 (2015) 4530–4536.

[78] S. Yu, Y. Wang, F. Sun, R. Wang, Y. Zhou, Novel mpg-C_3N_4/TiO_2 nanocomposite photocatalytic membrane reactor for sulfamethoxazole photodegradation, Chem. Eng. J., 337 (2018) 183–192.

[79] L. Chi, Y. Qian, J. Guo, X. Wang, H. Arandiyan, Z. Jiang, Novel g-C_3N_4/TiO_2/PAA/PTFE ultrafiltration membrane enabling enhanced antifouling and exceptional visible-light photocatalytic self-cleaning, Catal. Today, (2019), doi: https://doi.org/10.1016/j.cattod.2019.02.027, (In Press).

[80] H. Sun, G. Zhou, S. Liu, H.M. Ang, M.O. Tadé, S. Wang, Visible light responsive titania photocatalysts codoped by nitrogen and metal (Fe, Ni, Ag, or Pt) for remediation of aqueous pollutants, Chem. Eng. J., 231 (2013) 18–25.

[81] K. Govindan, S. Murugesan, P. Maruthamuthu, Photocatalytic degradation of pentachlorophenol in aqueous solution by visible light sensitive N–F-codoped TiO_2 photocatalyst, Mater. Res. Bull., 48 (2013) 1913–1919.

[82] D.-G. Huang, S.-J. Liao, J.-M. Liu, Z. Dang, L. Petrik, Preparation of visible-light responsive N–F-codoped TiO_2 photocatalyst by a sol–gel-solvothermal method, J. Photochem. Photobiol., A, 184 (2006) 282–288.

[83] J.-W. Xu, Z.-D. Gao, K. Han, Y. Liu, Y.-Y. Song, Synthesis of magnetically separable $Ag_3PO_4/TiO_2/Fe_3O_4$ heterostructure with enhanced photocatalytic performance under visible light for photoinactivation of bacteria, ACS Appl. Mater. Interfaces, 6 (2014) 15122–15131.

[84] X. Cao, W. Jing, W. Xing, Y. Fan, Y. Kong, J. Dong, Fabrication of a visible-light response mesoporous TiO_2 membrane with superior water permeability via a weak alkaline sol–gel process, Chem. Commun., 47 (2011) 3457–3459.

[85] A.T. Kuvarega, N. Khumalo, D. Dlamini, B.B. Mamba, Polysulfone/N,Pd co-doped TiO_2 composite membranes for photocatalytic dye degradation, Sep. Purif. Technol., 191 (2018) 122–133.

[86] W. Chen, T. Ye, H. Xu, T. Chen, N. Geng, X. Gao, An ultrafiltration membrane with enhanced photocatalytic performance from grafted N–TiO_2/graphene oxide, RSC Adv., 7 (2017) 9880–9887.

[87] H. Xu, M. Ding, S. Liu, Y. Li, Z. Shen, K. Wang, Preparation and characterization of novel polysulphone hybrid ultrafiltration membranes blended with N-doped GO/TiO_2 nanocomposites, Polymer, 117 (2017) 198–207.

[88] Y. Chen, W. Huang, D. He, S. Yue, H. Huang, Construction of heterostructured g-C_3N_4/Ag/TiO_2 microspheres with enhanced photocatalysis performance under visible-light irradiation, ACS Appl. Mater. Interfaces, 6 (2014) 14405–14414.

[89] H. Xu, M. Ding, W. Chen, Y. Li, K. Wang, Nitrogen–doped GO/TiO_2 nanocomposite ultrafiltration membranes for improved photocatalytic performance, Sep. Purif. Technol., 195 (2018) 70–82.

[90] C. Wang, C. Shao, L. Wang, L. Zhang, X. Li, Y. Liu, Electrospinning preparation, characterization and photocatalytic properties of Bi_2O_3 nanofibers, J. Colloid Interface Sci., 333 (2009) 242–248.

[91] S.S. Dunkle, R.J. Helmich, K.S. Suslick, $BiVO_4$ as a visible-light photocatalyst prepared by ultrasonic spray pyrolysis, J. Phys. Chem. C, 113 (2009) 11980–11983.

[92] U. Sulaeman, H. Pratiwi, A. Riapanitra, P. Iswanto, S. Yin, T. Sato, Hydrothermal synthesis and photocatalytic properties of $BiPO_4$/Ag_3PO_4 heterostructure for phenol decomposition, Adv. Mater. Res., 911 (2014) 92–96.

[93] H. Li, Y. Cui, W. Hong, High photocatalytic performance of $BiOI/Bi_2WO_6$ toward toluene and reactive brilliant red, Appl. Surf. Sci., 264 (2013) 581–588.

[94] M. Takeuchi, H. Yamagawa, M. Matsuoka, M. Anpo, Photocatalytic oxidation of acetaldehyde by hybrid Pt/WO_3–MOR photocatalysts under visible or sunlight irradiation, Res. Chem. Intermed., 40 (2014) 23–31.

[95] A. Tanaka, K. Hashimoto, H. Kominami, Visible-light-induced hydrogen and oxygen formation over Pt/Au/WO_3 photocatalyst utilizing two types of photoabsorption due to surface plasmon resonance and band-gap excitation, J. Am. Chem. Soc., 136 (2014) 586–589.

[96] T. Belin, N. Millot, N. Bovet, M. Gailhanou, In situ and time resolved study of the γ/α-Fe_2O_3 transition in nanometric particles, J. Solid State Chem., 180 (2007) 2377–2385.

[97] Y. Tong, L. Lu, X. Yang, X. Wang, Characterization and their photocatalytic properties of $Ln_2Zr_2O_7$ (Ln = La, Nd, Sm, Dy, Er) nanocrystals by stearic acid method, Solid State Sci., 10 (2008) 1379–1383.

[98] L. Zhou, Y. Tao, L. Du, W. Zhang, Role of calcination on sol-gel synthesis of porous $Sm_2Ti_2O_7$ for photocatalytic decolorization of RBR X-3B, Curr. Nanosci., 13 (2017) 506–512.

[99] S. Qian, Porous CuO hollow microspheres: one-step preparation and photocatalytic performance, Chin. J. Inogr. Chem., 28 (2012) 1043–1049.

[100] P.H. Lin, X.H. Du, Y.H. Chen, H.C. Chen, J.C. Huang, Nanoscaled diffusional or dislocation creep analysis of single-crystal ZnO, AIP Adv., 6 (2016) 095125.

[101] Q. Shao, M.C. Yang, G.E. Sheng-Song, W.U. Ya-Lin, Y.Y. Wang, L.W. Bao, Polystyrene-assisted hydrothermal preparation of ZnO tubes with high photocatalytic activity, Chin. J. Inogr. Chem., 30 (2014) 2601–2606.

[102] X. Hao, Y. Wang, J. Zhou, Z. Cui, Y. Wang, Z. Zou, Zinc vacancy-promoted photocatalytic activity and photostability of ZnS for efficient visible-light-driven hydrogen evolution, Appl. Catal., B, 221 (2018) 302–311.

[103] M. Saranya, R. Ramachandran, E.J.J. Samuel, S.K. Jeong, A.N. Grace, Enhanced visible light photocatalytic reduction of organic pollutant and electrochemical properties of CuS catalyst, Powder Technol., 279 (2015) 209–220.

[104] R. Chen, P. Wang, J. Chen, C. Wang, Y. Ao, Synergetic effect of MoS_2 and MXene on the enhanced H_2 evolution performance of CdS under visible light irradiation, Appl. Surf. Sci., 473 (2019) 11–19.

[105] P. Huo, C. Liu, D. Wu, J. Guan, J. Li, H. Wang, Q. Tang, X. Li, Y. Yan, S. Yuan, Fabricated Ag/Ag_2S/reduced graphene oxide composite photocatalysts for enhancing visible light photocatalytic and antibacterial activity, J. Ind. Eng. Chem., 57 (2018) 125–133.

[106] X. Zhang, Z. Ai, A. Falong Jia, L. Zhang, Generalized one-pot synthesis, characterization, and photocatalytic activity of hierarchical BiOX (X = Cl, Br, I) nanoplate microspheres, J. Phys. Chem. C, 112 (2008) 747–753.

[107] Z. Shan, W. Wang, X. Lin, H. Ding, F. Huang, Photocatalytic degradation of organic dyes on visible-light responsive photocatalyst $PbBiO_2Br$, J. Solid State Chem., 181 (2008) 1361–1366.

[108] B. Zhang, G. Ji, Y. Liu, M.A. Gondal, X. Chang, Efficient adsorption and photocatalytic pceerformance of flower-like three-dimensional (3D) I-doped BiOClBr photocatalyst, Catal. Commun., 36 (2013) 25–30.

[109] E. Zhang, L. Wang, B. Zhang, Y. Xie, C. Sun, C. Chen, Y. Zhang, G. Wang, Modification of polyvinylidene fluoride membrane with different shaped α-Fe_2O_3 nanocrystals for enhanced photocatalytic oxidation performance, Mater. Chem. Phys., 214 (2018) 41–47.

[110] R. Singh, V.S.K. Yadav, M.K. Purkait, Cu_2O photocatalyst modified antifouling polysulfone mixed matrix membrane for ultrafiltration of protein and visible light driven photocatalytic pharmaceutical removal, Sep. Purif. Technol., 212 (2019) 191–204.

[111] J. Madhavan, F. Grieser, M.A. Kumar, Combined advanced oxidation processes for the synergistic degradation of ibuprofen in aqueous environments, J. Hazard. Mater, 178 (2010) 202–208.

[112] M. Kazemi, M. Jahanshahi, M. Peyravi, Chitosan-sodium alginate multilayer membrane developed by Fe^0@WO_3 nanoparticles: Photocatalytic removal of hexavalent chromium, Carbohydr. Polym., 198 (2018) 164–174.

[113] S.N. Ramanan, N. Shahkaramipour, T. Tran, L. Zhu, S.R. Venna, C.-K. Lim, A. Singh, P.N. Prasad, H. Lin, Self-cleaning membranes for water purification by co-deposition of photo-mobile 4,4′-azodianiline and bio-adhesive polydopamine, J. Membr. Sci., 554 (2018) 164–174.

[114] M.A. Mohamed, W.N.W. Salleh, J. Jaafar, A.F. Ismail, M.A. Mutalib, N.A.A. Sani, S.E.A.M. Asri, C.S. Ong, Physicochemical characteristic of regenerated cellulose/N-doped TiO_2 nanocomposite membrane fabricated from recycled newspaper with photocatalytic activity under UV and visible light irradiation, Chem. Eng. J., 284 (2016) 202–215.

[115] X. Wu, J. Cheng, X. Li, K. Lv, Enhanced visible photocatalytic oxidation of NO by repeated calcination of g-C_3N_4, Appl. Surf. Sci., 465 (2019) 1037–1046.

[116] S. Yu, J. Liu, W. Zhu, Z.T. Hu, T.T. Lim, X. Yan, Facile room-temperature synthesis of carboxylated graphene oxide-copper sulfide nanocomposite with high photodegradation and

disinfection activities under solar light irradiation, Sci. Rep., 5 (2015) 16369.

[117] C. Hu, M.-S. Wang, C.-H. Chen, Y.-R. Chen, P.-H. Huang, K.-L. Tung, Phosphorus-doped g-C$_3$N$_4$ integrated photocatalytic membrane reactor for wastewater treatment, J. Membr. Sci., 580 (2019) 1–11.

[118] Y. Xiaoju, B. Ruiling, Y. Shuili, Effect of inorganic ions on the photocatalytic degradation of humic acid, Russ. J. Phys. Chem. A, 86 (2012) 1318–1325.

[119] H. Song, J. Shao, Y. He, J. Hou, W. Chao, Natural organic matter removal and flux decline with charged ultrafiltration and nanofiltration membranes, J. Membr. Sci., 376 (2011) 179–187.

[120] A. Rajeswari, S. Vismaiya, A. Pius, Preparation, characterization of nano ZnO-blended cellulose acetate-polyurethane membrane for photocatalytic degradation of dyes from water, Chem. Eng. J.,313 (2017) 928–937.

[121] C.P. Athanasekou, S. Morales-Torres, V. Likodimos, G.E. Romanos, L.M. Pastrana-Martinez, P. Falaras, D.D. Dionysiou, J.L. Faria, J.L. Figueiredo, A.M.T. Silva, Prototype composite membranes of partially reduced graphene oxide/TiO$_2$ for photocatalytic ultrafiltration water treatment under visible light, Appl. Catal., B, 158–159 (2014) 361–372.

[122] G. Liu, K. Han, H. Ye, C. Zhu, Y. Gao, Y. Liu, Y. Zhou, Graphene oxide/triethanolamine modified titanate nanowires as photocatalytic membrane for water treatment, Chem. Eng. J., 320 (2017) 74–80.

[123] S.K. Papageorgiou, F.K. Katsaros, E.P. Favvas, G. Em. Romanos, C.P. Athanasekou, K.G. Beltsios, O.I. Tzialla, P. Falaras, Alginate fibers as photocatalyst immobilizing agents applied in hybrid photocatalytic/ultrafiltration water treatment processes, Water Res., 46 (2012) 1858–1872.

[124] N.E. Salim, J. Jaafar, A.F. Ismail, M.H.D. Othman, M.A. Rahman, N. Yusof, M. Qtaishat, T. Matsuura, F. Aziz, W.N.W. Salleh, Preparation and characterization of hydrophilic surface modifier macromolecule modified poly (ether sulfone) photocatalytic membrane for phenol removal, Chem. Eng. J., 335 (2018) 236–247.

[125] S. Chakraborty, S. Loutatidou, G. Palmisano, J. Kujawa, M.O. Mavukkandy, S. Al-Gharabli, E. Curcio, H.A. Arafat, Photocatalytic hollow fiber membranes for the degradation of pharmaceutical compounds in wastewater, J. Environ. Chem. Eng., 5 (2017) 5014–5024.

[126] K.V. Plakas, V.C. Sarasidis, S.I. Patsios, D.A. Lambropoulou, A.J. Karabelas, Novel pilot scale continuous photocatalytic membrane reactor for removal of organic micropollutants from water, Chem. Eng. J., 304 (2016) 335–343.

[127] K. Szymański, A.W. Morawski, S. Mozia, Humic acids removal in a photocatalytic membrane reactor with a ceramic UF membrane, Chem. Eng. J., 305 (2016) 19–27.

[128] A. Oun, N. Tahri, S. Mahouche-Chergui, B. Carbonnier, S. Majumdar, S. Sarkar, G.C. Sahoo, R. Ben Amar, Tubular ultrafiltration ceramic membrane based on titania nanoparticles immobilized on macroporous clay-alumina support: elaboration, characterization and application to dye removal, Sep. Purif. Technol., 188 (2017) 126–133.

[129] N.G. Moustakas, F.K. Katsaros, A.G. Kontos, G.E. Romanos, D.D. Dionysiou, P. Falaras, Visible light active TiO$_2$ photocatalytic filtration membranes with improved permeability and low energy consumption, Catal. Today, 224 (2014) 56–69.

[130] X.Q. Li, W.X. Zhang, Sequestration of metal cations with zerovalent iron nanoparticles-a study with high resolution X-ray photoelectron spectroscopy (HR-XPS), J. Phys. Chem. C, 111 (2007) 6939–6946.